TipESM

Exploring Tipping Points and Their Impacts Using Earth System Models

# Storm and flood data

Deliverable D6.1

Funded by the European Union

UK Research and Innovation

UK Partners are funded by UK Research and Innovation (UKRI) under the UK government's Horizon Europe funding Guarantee.

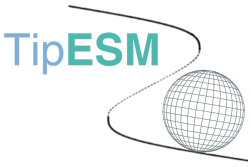


**About this document**

**First submission date to the European Commission:** 28 August 2025 (first submission)

**Revised on:** 30 April 2026**,** in section 2.1.3 Sampling of storms with integrations on the formulae.

**Revised on:** 8 October 2025, with integrations in section 2.2.4 by the authors.

**Revision on:** 29 October 2025, with a small integration in section 2.1.2 by the authors.

**Dissemination Level:** Public (PU)

**Work package**: WP6 Climate-driven tipping of ecological and social systems

**Authors**:

Potsdam-Institut für Klimafolgenforschung e.V. (PIK), PP6, Jacob Schewe, jacob.schewe@pik-potsdam.de; Dánnell Quesada Chacón, Sandra Zimmermann

**Contributors:**

Potsdam-Institut für Klimafolgenforschung e.V. (PIK), PP6, Jan Volkholz, Inga Sauer

**Reviewer:**

Danish Meteorological Institute (DMI), PP1, Chiara Bearzotti chb@dmi.dk

**Disclaimer**: Funded by the European Union. Views and opinions expressed are however those of the author(s) only and do not necessarily reflect those of the European Union or the European Climate, Infrastructure and Environment Executive Agency (CINEA). Neither the European Union nor the granting authority can be held responsible for them.

# TABLE OF CONTENTS

# 1. Abstract

This deliverable describes the datasets of areas affected by strong tropical cyclone winds and flooded areas made accessible through the ISIMIP data repository. These datasets are derived from state-of-the-art climate, tropical cyclone, hydrological, and hydrodynamic model simulations, respectively, prepared in the context of CMIP6 and ISIMIP3. They describe the annual maximum storm intensity (in terms of wind speed) and flooded area fraction, respectively, in each grid cell globally, under historical and future climatic conditions, according to different scenarios of greenhouse gas concentrations. The data can be used for assessing the risks associated with these two hazards, such as risks to life, livelihoods, health, or economic assets. In the context of TipESM, they support the assessment of potential tipping dynamics in household recovery from climate-induced shocks and related poverty risks, as well as flood-induced human displacement risk.

# 2. Work Done

## 2.1 Storm data

The storm data were produced according to the methodology presented below. The methodology represents a reproducible, bias-adjusted workflow for generating tropical cyclone (TC) windfield datasets, based on a sampling approach. The aim is to ensure that the statistical properties of simulated TC windfields closely align with observations, while allowing extension across multiple climate models and scenarios.

### 2.1.1 Data sources

Observed TC tracks are sourced from the IBTrACS archive, which provides storm center positions from 1851 to present-day records. Simulated TC tracks are derived from WindRiskTech's global synthetic datasets (Emanuel et al., 2008), utilising boundary conditions such as sea surface temperature, air temperature, and winds at height, from five global climate models (GCMs) and up to six experiments. Each available model-experiment combination includes 1500 synthetic tracks per year. However, not all combinations are

available for the full duration of the respective experiments, and coverage varies by model and scenario. See Tab. 1 for further details.

**Table 1:** Available simulated tropical cyclone tracks per GCM, experiment, and period. The data is provided by WindRiskTech.

| GCM | Experiment | Period |
|---|---|---|
| GFDL-ESM4 | Historical | 1850–2014 |
| GFDL-ESM4 | ssp585 | 2061–2100 |
| IPSL-CM6A-LR | Historical | 1850–2014 |
| IPSL-CM6A-LR | piControl | 1850–2014 |
| IPSL-CM6A-LR | ssp126 | 2061–2100 |
| IPSL-CM6A-LR | ssp245 | 2015–2100 |
| IPSL-CM6A-LR | ssp370 | 2015–2100 |
| IPSL-CM6A-LR | ssp585 | 2015–2100 |
| MPI-ESM1-2-HR | Historical | 1850–2014 |
| MPI-ESM1-2-HR | piControl | 1850–2014 |
| MPI-ESM1-2-HR | ssp126 | 2061–2100 |
| MPI-ESM1-2-HR | ssp245 | 2015–2100 |
| MPI-ESM1-2-HR | ssp370 | 2015–2100 |
| MPI-ESM1-2-HR | ssp585 | 2015–2100 |
| MRI-ESM2-0 | Historical | 1950–2014 |
| MRI-ESM2-0 | piControl | 1850–2014 |
| MRI-ESM2-0 | ssp126 | 2061–2100 |
| MRI-ESM2-0 | ssp245 | 2015–2100 |
| MRI-ESM2-0 | ssp370 | 2015–2100 |
| MRI-ESM2-0 | ssp585 | 2015–2100 |
| UKESM1-0-LL | Historical | 1850–2014 |
| UKESM1-0-LL | piControl | 1960–2100 |
| UKESM1-0-LL | ssp126 | 2061–2100 |
| UKESM1-0-LL | ssp245 | 2015–2100 |
| UKESM1-0-LL | ssp370 | 2015–2100 |
| UKESM1-0-LL | ssp585 | 2015–2100 |

### 2.1.2 Wind field calculation

Both observed and simulated tracks are converted into windfields using the Holland (2008) parametric model, as implemented in the *climada* Python package (Siguan et al., 2023). Windfield generation is performed for all grid cells located over land and for those over the ocean within 50 km of the coastline, at a spatial resolution of 300 arcseconds (~0.0833°). The fields are computed up to a radial distance of 1,500 km from the storm centre. A wind speed threshold of 17.5 m/s (34 knots), corresponding to the tropical storm classification on the Saffir-Simpson scale, is applied; i.e., grid cells where wind speed is estimated to be lower than this threshold are considered unaffected, and their wind speed is set to zero. All subsequent filtering and wind speed thresholds are applied directly to the windfields rather than the original tracks, ensuring consistency throughout the workflow.

### 2.1.3 Sampling of storms

To produce regionally meaningful datasets, these global windfields are further processed on a subbasin basis. This step involves bias-adjusting the windfield statistics for each region to account for differences in climatology, observational coverage, and data quality. Subbasin-specific adjustment ensures that the final statistics accurately reproduce observed TC characteristics within each region during the historical period. The procedure is similar to that described in Geiger et al. (2021).

Bias correction is applied to the timeseries of both event counts and mean intensities, using normalization periods tailored to each subbasin: West Pacific (WP, 1950-2015), North Atlantic (NA, 1950-2015), East Pacific (EP, 1950-2015), North Indian (NI, 1980-2015), South Indian (SI, 1980-2015), South Pacific (SP, 1980-2015), and South Atlantic (SA, 1980-2015). For each basin, the simulated event count is scaled by the ratio of the sums of observed to simulated events over the normalisation period $\alpha = \frac{\Sigma\, Events_{obs}}{\Sigma\, Events_{sim}}$. Similarly, mean intensity (i.e., each storm's maximum wind speed over land, averaged over all storms during the normalisation period) and the intensity's standard deviation are scaled using the ratio of observed to simulated corresponding values, $\beta = \frac{\overline{Intensity_{obs}}}{\overline{Intensity_{sim}}}$ and $\gamma = \frac{\sigma(Intensity_{obs})}{\sigma(Intensity_{sim})}$ respectively. This approach ensures alignment with both the average frequency and intensity of observed TCs in each subbasin.

Given an uncalibrated number of events $n$ for each year and basin, the calibrated expected global annual event count $freqyear$, the uncalibrated global total number of 1500 simulated tracks per year, and the

bias-adjustment factors described above, a bias-corrected expected basin-wise annual event count $\widehat{N}$ is calculated: $\widehat{N} = n \cdot \alpha \cdot \frac{freqyear}{1500}$. To reflect the probabilistic nature of TC occurrence, 100 independent realisations are generated per year. In each realisation, the number of events $N$ is drawn from a Poisson distribution with the expected value set to the bias-adjusted mean event count $\widehat{N}$. $N$ events are then randomly sampled from the pool of precomputed windfields corresponding to that basin and year. The mean intensity of this set of $N$ events should be between the range $\left[\widehat{Intensity}_{mean} - \widehat{Intensity}_{std}, \widehat{Intensity}_{mean} + \widehat{Intensity}_{std}\right]$, where $\widehat{Intensity}_{mean} = \beta \cdot Intensity_{mean}$ and $\widehat{Intensity}_{std} = \gamma \cdot Intensity_{std}$ while the bias-adjusted standard deviation of the intensity should be between 0.5 and 10 m/s. If the set does not satisfy these conditions, it is discarded, and a new set is drawn. If no suitable event set is found after 10,000 iterations, the aforementioned acceptable intensity range is expanded by ±1 m/s. This process is repeated until 100 realisations have been generated.

This basin-wise dataset was then aggregated to indicate the yearly maximum windspeed per pixel per realisation, and the basins were merged into a global grid. This final dataset is saved in NetCDF format. The workflow is modular and fully parameterised, supporting straightforward adaptation to additional GCMs, experiments, resolutions, or regions.

## 2.2 Flood data

The flood data were produced according to the following methodology:

### 2.2.1 Hydrological modelling

The data is derived from river runoff simulations using multiple global hydrological models (GHMs), driven by atmospheric forcing from global climate models, in the framework of ISIMIP3b (Frieler et al., 2025). Daily runoff was simulated globally on a 0.5° horizontal grid for pre-industrial, historical, and projected future conditions, according to different Shared Socioeconomic Pathways (SSPs; Riahi et al., 2017). Table 2 lists the GHMs, GCMs, and SSPs used. Note that not all combinations of GHM, GCM, and SSP were simulated.

**Table 2:** Models and scenarios for which flood data are available.

| GHMs | GCMs | Scenarios |
|---|---|---|
| CLASSIC | gfdl-esm4, ukesm1-0-II | historical, picontrol, ssp126, ssp370, ssp585 |
| CWatM | ukesm1-0-II, gfdl-esm4, ipsl-cm6a-lr, mpi-esm1-2-hr, mri-esm2-0, ukesm1-0-II | historical, picontrol, ssp126, ssp370, ssp585 |
| H08 | ukesm1-0-II, gfdl-esm4, ipsl-cm6a-lr, mpi-esm1-2-hr, mri-esm2-0, ukesm1-0-II | historical, picontrol, ssp126, ssp370, ssp585 |
| JULES-W2 | ukesm1-0-II, gfdl-esm4, ipsl-cm6a-lr, mpi-esm1-2-hr, mri-esm2-0, ukesm1-0-II | historical, picontrol, ssp126, ssp370, ssp585 |
| MIROC-INTEG-LAND | ukesm1-0-II, gfdl-esm4, ipsl-cm6a-lr, mpi-esm1-2-hr, mri-esm2-0, ukesm1-0-II | historical, picontrol, ssp126, ssp370, ssp585 |
| WaterGAP2-2e | ukesm1-0-II, gfdl-esm4, ipsl-cm6a-lr, mpi-esm1-2-hr, mri-esm2-0, ukesm1-0-II | historical, picontrol, ssp126, ssp370, ssp585 |
| WEB-DHM-SG | ukesm1-0-II, gfdl-esm4, ipsl-cm6a-lr, mpi-esm1-2-hr, mri-esm2-0, ukesm1-0-II | historical, picontrol, ssp126, ssp370, ssp585 |

### 2.2.2 Hydrodynamic modelling

Daily runoff was interpolated horizontally from the 0.5° ISIMIP grid to CaMa-Flood's unit catchments (using a map, inpmat-30min.bin, included with the model code) and then routed through the global hydrodynamic model CaMa-Flood (Yamazaki et al., 2011), version 4.0.0. The resulting daily river discharge at 0.25° resolution then served as a basis for the inundation modelling. The annual maximum flood depth at each grid cell was determined, resulting in a yearly estimate of maximum flood depth (above river channel), and associated flooded area fraction, at 0.25° resolution.

### 2.2.3 Accounting for flood protection

A generalised extreme value distribution (GEV; Willner et al., 2018) was fit to the pre-industrial distribution of daily discharge, separately at each grid cell. From this fit, the return period associated with any given discharge level was determined in both historical and future simulations. This allowed us to produce flood estimates that accounted for different levels of assumed flood protection by masking out flooding in grid cells and years in which the annual maximum discharge was below the return period against which that grid cell was assumed to be protected. Table 2 describes the different flood protection assumptions.

**Table 3:** Flood protection assumptions.

| File name specifier | Explanation |
|---|---|
| none | no flood protection |
| 2y | protection against floods with a pre-industrial return period of 2 years or shorter |
| 40y | protection against floods with a pre-industrial return period of 40 years or shorter |
| flopros | protection standards according to the merged layer of FLOPROS (Scussolini et al., 2016) |
| hanze | protection standards according to HANZE within Europe (Paprotny et al., 2023) and FLOPROS for the rest of the world |

### 2.2.4 Flooded fraction

The final usable result is the flooded area fraction at 0,25° horizontal resolution. This relates to the fraction of a unit catchment that is inundated. Each unit catchment corresponds to a 0.25° x 0.25° grid cell but is irregularly shaped, which means that the flood fraction does not precisely represent the inundated fraction of the grid cell; this should be kept in mind when analysing the data.

# 3. Results Achieved

The datasets, produced according to the methodologies described above, are publicly available:

- Storm data: Dánnell Quesada-Chacón (2025): Global projections of tropical cyclones based on the ISIMIP3b ensemble of global climate models: maximum wind speed (v1.0). **ISIMIP Repository**. https://doi.org/10.48364/ISIMIP.368090
- Flood data: Jan Volkholz, Sandra Zimmermann, Jan Hassel (2025): Global projections of fluvial floods based on the ISIMIP3b ensemble of global hydrological models: flooded area fraction (v1.0). **ISIMIP Repository.** https://doi.org/10.48364/ISIMIP.294944

# 4. Contribution to the TipESM objectives

This deliverable contributes to achieving the following project-specific objectives (SO).

| | | |
|---|---|---|
| SO6 | To identify tipping events in ecological and societal systems, with a focus on the climate drivers of these events, emphasising biodiversity, human health and habitability. KPIs: A report detailing ecological and societal TPs and climate thresholds that may cause tipping. (Deliverables: D6.1, D6.2 and D6.3. Milestones: MS6 and MS7). | Work packages: 1,3,6 |
| This deliverable provides the necessary hazard projection data to assess tipping processes in societal systems, particularly regarding poverty and human displacement. | | |

# 5. References

Emanuel, K., Sundararajan, R., & Williams, J. (2008). Hurricanes and Global Warming: Results from Downscaling IPCC AR4 Simulations. *Bulletin of the American Meteorological Society*, *89*(3), 347–368. https://doi.org/10.1175/BAMS-89-3-347

Frieler et al. Scenario set-up and the new CMIP6-based climate-related forcings provided within the third round of the Inter-Sectoral Model Intercomparison Project (ISIMIP3b, group I and II), EGUsphere [preprint], https://doi.org/10.5194/egusphere-2025-2103, 2025.

Geiger, T., Gütschow, J., Bresch, D. N., Emanuel, K., & Frieler, K. (2021). Double benefit of limiting global warming for tropical cyclone exposure. *Nature Climate Change*, *11*(10), 861–866. https://doi.org/10.1038/s41558-021-01157-9

Holland, G. (2008). A Revised Hurricane Pressure–Wind Model. *Monthly Weather Review*, *136*(9), 3432–3445. https://doi.org/10.1175/2008MWR2395.1

Paprotny, D., Mengel, M. Population, land use, and economic exposure estimates for Europe at 100 m resolution from 1870 to 2020. *Sci Data* **10**, 372 (2023). https://doi.org/10.1038/s41597-023-02282-0

Riahi, K., van Vuuren, D. P., Kriegler, E., Edmonds, J., O'Neill, B. C., Fujimori, S., Bauer, N., Calvin, K., Dellink, R., Fricko, O., Lutz, W., Popp, A., Cuaresma, J. C., KC, S., Leimbach, M., Jiang, L., Kram, T., Rao, S., Emmerling, J., … Tavoni, M. (2017). The Shared Socioeconomic Pathways and their energy, land use, and greenhouse gas emissions implications: An overview. *Global Environmental Change*, *42*, 153–168. https://doi.org/10.1016/j.gloenvcha.2016.05.009

Scussolini, P., Aerts, J. C. J. H., Jongman, B., Bouwer, L. M., Winsemius, H. C., de Moel, H., & Ward, P. J. (2016). FLOPROS: an evolving global database of flood protection standards. *Natural Hazards and Earth System Sciences*, *16*(5), 1049–1061. https://doi.org/10.5194/nhess-16-1049-2016

Siguan, G. A., Schmid, E., Vogt, T., Eberenz, S., Steinmann, C. B., Röösli, T., Yu, Y., Mühlhofer, E., Lüthi, S., Sauer, I. J., Hartman, J., Kropf, C. M., Guillod, B. P., Stalhandske, Z., Ciullo, A., Bresch, D. N., Riedel, L., Fairless, C., Schmid, T., … scem. (2023). *CLIMADA-project/climada_python: V4.0.1* [Computer software]. Zenodo. https://doi.org/10.5281/zenodo.8383171

Willner, S. N., Levermann, A., Zhao, F., & Frieler, K. (2018). Adaptation required to preserve future high-end river flood risk at present levels. *Science advances*, *4*(1), eaao1914. https://doi.org/10.1126/sciadv.aao1914

Yamazaki, D., Kanae, S., Kim, H., & Oki, T. (2011). A physically based description of floodplain inundation dynamics in a global river routing model. *Water Resources Research*, *47*(4), 2010WR009726. https://doi.org/10.1029/2010WR009726